Delay-induced synchrony in complex networks with conjugate coupling

M. Manju Shrii,[1,2] D. V. Senthilkumar,[2] and J. Kurths[1,2,3]
[1]*Institute for Physics, Humboldt University, 12489 Berlin, Germany*
[2]*Potsdam Institute for Climate Impact Research, 14473 Potsdam, Germany*
[3]*Institute for Complex Systems and Mathematical Biology, University of Aberdeen, United Kingdom*
(Received 8 December 2011; revised manuscript received 1 March 2012; published 22 May 2012)

We demonstrate stable synchronous chaos in a delay coupled network of time continuous dynamical system using the framework of master stability formalism (MSF). It is further shown that conjugate coupling, i.e., coupling using dissimilar variables, can substitute delay coupling of similar variables in retrieving delay-induced phenomena. By exploiting the MSF, we show that delayed conjugate coupling in an arbitrary network is capable of both inducing synchronization where there is no synchronization at all and enhancing synchronization to a large parameter space, which even the conjugate coupling without delay is incapable of. The above results are demonstrated using the paradigmatic Rössler system and Hindmarsh-Rose neuron.

DOI: 10.1103/PhysRevE.85.057203 PACS number(s): 05.45.Xt, 02.30.Ks, 89.75.−k

Connection delays unveil a plethora of collective (self-organized) dynamical behavior of a network of coupled dynamical systems which the isolated units are incapable of. Examples include hysteresis, phase locking, phase flip, amplitude death, multistable states, chimera states [1,2]. Synchronization is a fundamental nonlinear phenomenon exhibited by such a network of coupled dynamical systems with applications branching out into a vast areas of science and technology [3–5]. Investigating nontrivial effects of homogeneous and/or heterogeneous connection delays, network topology, diversity in connections, and in dynamical systems on synchronizability of networks have received an immense importance in recent research [3–7].

The master stability formalism (MSF) [8] has been widely exploited in probing the stability of synchronization from regular to complex networks [3–5]. Nevertheless, only a very few recent investigations have employed the MSF in investigating the stability of synchronization in delay-coupled networks [7,9,10], in which the analyses are restricted to either map or phase oscillators except in Ref. [7]. Nevertheless, the authors of Ref. [7] admitted that their analysis could not establish stable synchronized states in the master stability surface of the network of delay coupled HR neurons. Hence the framework of MSF has not yet been successfully employed in determining the stability of delay coupled networks of time continuous dynamical systems.

In this Brief Report, we employ the MSF in probing the stable synchronized states in an arbitrary network with delayed conjugate (dissimilar) coupling by considering the paradigmatic models of the Rössler system [11–13] and the Hindmarsh-Rose (HR) neuron [7,12,14]. Conjugate coupling corresponds to a coupling via a dissimilar variable and has been widely employed [15,16]. A conjugate variable $y(t)$ can be viewed as a delayed version, $y(t) = x(t-\tau)$, of an observable $x(t)$ in accordance with the Takens' embedding theorem [17] and hence a conjugate coupling can substitute the delay coupling of a similar variable in achieving the delay-induced dynamical behaviors. For instance, it has been shown that amplitude death can be achieved in identical oscillators with conjugate coupling without any delay [15].

By using the MSF, we will show that the delayed conjugate coupling is capable of both inducing synchronization where there is no synchronization at all without delay and enhancing the existing synchronization to a large parameter space in an arbitrary network. We would like to emphasize that as a conjugate coupling can substitute the delayed coupling of similar variables in retrieving delay-induced phenomena as mentioned above, the delayed conjugate coupling can even outperform the conjugate coupling without delay in provoking rich dynamical behaviors. To the best of our knowledge, none of the existing studies have shown stable synchronous chaos, in particular along with the phenomenon of delay-induced and delay-enhanced synchronization, in a delay coupled network of a time continuous system using the MSF.

In particular, we will show that the delayed conjugate couplings $[x(t-\tau) \rightarrow y(t-\tau)$ and $y(t-\tau) \rightarrow x(t-\tau)]$ can induce stable synchronous chaos in a network of Rössler oscillators, whereas the same couplings without delay do not show any synchrony at all. On the other hand, the delayed conjugate couplings in a network of HR neurons enhance the existing synchronization to a large parameter range. Further, synchronization can also be achieved even for smaller coupling strengths than that without delay in the conjugate coupling. As a conjugate variable can be viewed as the delayed version of an observable $x(t)$, delayed conjugate coupling may be considered as coupling of the observable with further larger delays, i.e., $y(t-\tau) = x(t-2\tau)$. Consequently, this may explain the limitation on the maximum delay to be less than the time scale of the dynamical system to induce stable synchronization [10] and may open up the possibility to account for long-range neural synchrony in the central nervous system [7,18], long-range spatial synchronization in ecology [19], in climatology [20], in laser physics [21], to name a few; this needs further investigation and remains an open problem. We will also establish the stable synchronized regime in the complex plane of the MSF from the values of the largest transverse Lyapunov exponent of the transverse modes of the delay-coupled network.

We consider an arbitrary delay-coupled network with N identical chaotic units in accordance with the MSF [8] as follows:

$$\dot{x}_i(t) = f[x_i(t)] - \sigma \sum_{j=1}^{N} g_{ij} h[x_j(t-\tau)], \quad (1)$$

where $x_i \in \mathbb{R}^m, i = 1, \ldots, N$, f is a nonlinear function describing the dynamics of the individual units, σ is the overall coupling strength, $G = g_{ij}$ is a $N \times N$ matrix, which determines the topology of an arbitrary network, h is a linear coupling function and the corresponding Jacobian matrix $Dh_{12,21} = 1$ for conjugate couplings while other elements are zero, and τ is the coupling delay. The invariant synchronization manifold is assured by the zero row sum, that is $\sum_{j=1}^{N} g_{ij} = 0 \forall i$, of each row of the connectivity matrix G. If G is diagonalizable, then the stability of the synchronization manifold is governed by the eigenvalues of G and the following block diagonalized variational equation for the transverse modes

$$\dot{\xi}(t) = Df[x(t)]\xi(t) - \varepsilon Dh[x(t-\tau)]\xi(t-\tau). \quad (2)$$

Here, $x(t)$ is the dynamics within the synchronization manifold, $\xi(t)$ is a perturbation transverse to the synchronization manifold, which could be complex, $Df[x(t)]$ is the Jacobian evaluated on the synchronization manifold, and $Dh[x(t-\tau)]$ is an $m \times m$ matrix that determines which components of the oscillator are coupled. The normalized coupling parameter $\varepsilon = \sigma\gamma_k$, where γ_k is the kth eigenvalue of the coupling matrix G, $k = 0,1,2,\ldots,N-1$. It is to be noted that γ_k is more generic because G is arbitrary and it could be the eigenvalue corresponding to any specific topology determined by G. Here, $k = 0$ corresponds to the synchronization manifold with $\gamma_0 = 0$, while all the other eigenvalues for $k > 0$ correspond to the transverse modes determining the stability of the synchronization manifold $x(t)$. Thus the synchronized state is stable for a given network topology, characterized by G, when all the eigenvalues of G for $k > 0$ are negative [or when all the transverse Lyapunov exponents of (2) are negative]. Considering the fact that G could have complex eigenvalues $\varepsilon = \sigma\gamma_k = -(\alpha + i\beta)$, the generic variational equation, i.e., the MSF, can be written as

$$\dot{\xi}(t) = Df[x(t)]\xi(t) + (\alpha + i\beta)Dh[x(t-\tau)]\xi(t-\tau), \quad (3)$$

where, α and β are the real and imaginary parts of the eigenvalue. Separating $\xi(t)$ into the real part $\xi_r(t)$ and the imaginary part $\xi_i(t)$, we get

$$\dot{\xi}_r(t) = Df[x(t)]\xi_r(t) + \alpha Dh[x(t-\tau)]\xi_r(t-\tau) - \beta Dh[x(t-\tau)]\xi_i(t-\tau), \quad (4a)$$

$$\dot{\xi}_i(t) = Df[x(t)]\xi_i(t) + \alpha Dh[x(t-\tau)]\xi_i(t-\tau) + \beta Dh[x(t-\tau)]\xi_r(t-\tau). \quad (4b)$$

The maximal transverse Lyapunov exponent ($\lambda_{\max}$) estimated from Eqs. (4) yields a complex surface in the (α,β) plane, namely the master stability surface of the considered network of oscillators. For a given value of the coupling strength σ and the delay time τ, one can locate a point in the complex surface and the sign of $\lambda_{\max}$ at that point determines the stability of the synchronization manifold.

Next, we analyze the Rössler systems governed by the equation of motions [8,12,13] $\dot{x} = -y - z, \dot{y} = x + 0.2y, \dot{z} = 0.2 + z(x - 9.0)$ as nodes in the network with the delayed conjugate coupling, $x(t-\tau) \rightarrow y(t-\tau)$. The largest transverse Lyapunov exponent, estimated from the MSF (2), depicted in Fig. 1(a) for $\tau = 0$ indicates that the network is in an asynchronous state as $\lambda_{\max} > 0$ in the entire range of ε. In contrast, in the presence of a delay in the same conjugate coupling, the network of Rössler systems is entrained to synchronous oscillations as confirmed by the sign of $\lambda_{\max}$ in Fig. 1(a) for $\tau = 1.8$ attributing to the phenomenon of

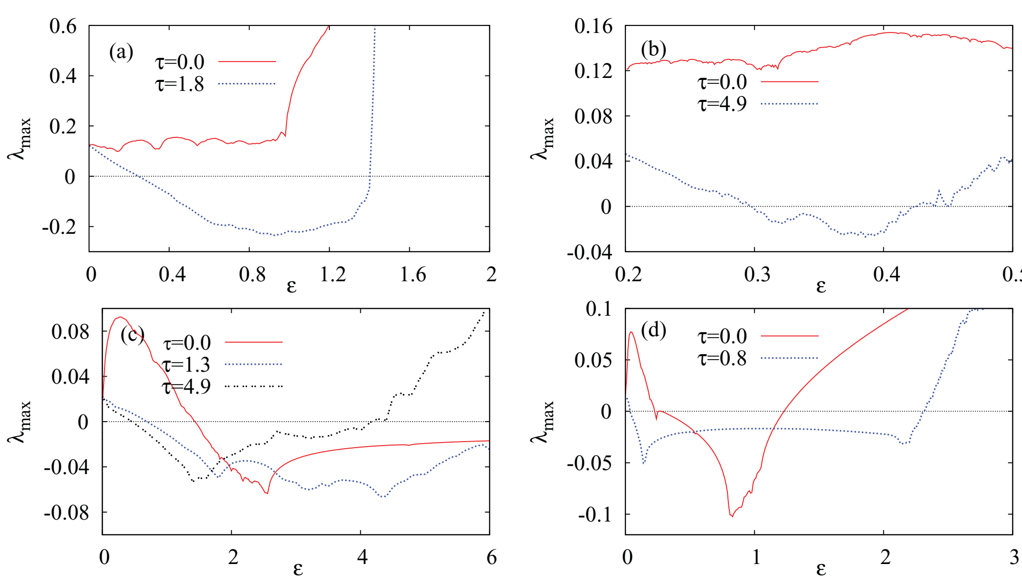

FIG. 1. (Color online) The largest transverse Lyapunov exponents $\lambda_{\max}$ of the MSF (2) of the delay-coupled network as a function of the normalized coupling parameter ε for different values of the delay τ in the conjugate coupling. (a) $x(t-\tau) \rightarrow y(t-\tau)$ coupled Rössler system for $\tau = 0.0$ and 1.8, (b) $y(t-\tau) \rightarrow x(t-\tau)$ coupled Rössler system for $\tau = 0.0$ and 4.9, (c) $x(t-\tau) \rightarrow y(t-\tau)$ coupled HR neurons for $\tau = 0.0$, 1.3, and 4.9, and (d) $y(t-\tau) \rightarrow x(t-\tau)$ coupled HR neurons for $\tau = 0.0$ and 0.8.

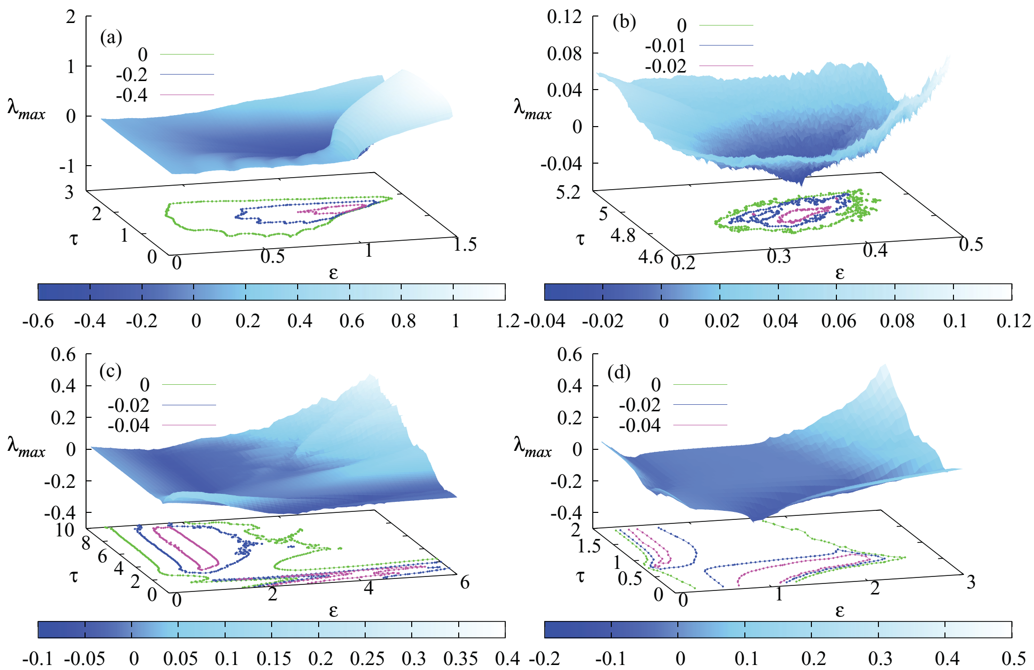

FIG. 2. (Color online) Surface of the largest transverse Lyapunov exponents $\lambda_{\max}$ as a function of the coupling delay τ and the normalized coupling parameter ε. An increase in the color density corresponds to a decrease in the value of $\lambda_{\max}$ and the contours encompasses the stable synchronized regime corresponding to $\lambda_{\max} < 0$. (a) $x(t-\tau) \to y(t-\tau)$ coupled Rössler system, (b) $y(t-\tau) \to x(t-\tau)$ coupled Rössler system, (c) $x(t-\tau) \to y(t-\tau)$ coupled HR neurons, and (d) $y(t-\tau) \to x(t-\tau)$ coupled HR neurons.

delay-induced synchronization in the network. The effect of delay coupling can be better understood from Fig. 2(a), where $\lambda_{\max}$ is shown as a surface in the (τ,ε) plane. An increase in the color intensity corresponds to a decrease in the $\lambda_{\max}$ and the isoclinic lines encompass the stable synchronous regime corresponding to the $\lambda_{\max} < 0$. It is evident from Fig. 2(a) that without delay in the coupling the network of Rössler systems does not exhibit any synchronous oscillation. On the other hand, as τ is increased the network attains synchronization after an appreciable delay and the range of stable synchronization increases with it up to a certain threshold. Further increase in the delay results in a decrease in the spread of stable synchronization and finally reaches asynchronization for further larger delays. The corresponding master stability surface, i.e., the surface of $\lambda_{\max}$ in the complex (α,β) plane, estimated from the MSF (4) is illustrated in Fig. 3(a) for the coupling delay $\tau = 1.8$, in which the stable regimes are displayed by the contours of $\lambda_{\max} < 0$.

A similar result is also observed for another choice of the delayed conjugate coupling, namely $y(t-\tau) \to x(t-\tau)$. The sign of $\lambda_{\max}$ [see Fig. 1(b)] as a function of ε for both with and without delay in the conjugate coupling asserts the phenomenon of delay-induced synchronization in the network of Rössler systems. The surface of $\lambda_{\max}$ in Fig. 2(b) and its contours for $\lambda_{\max} < 0$ clearly illustrates the above phenomenon. Further, the complex (α,β) plane of the MSF in Fig. 3(b) for $\tau = 4.9$ with $\lambda_{\max} < 0$ confirms the same.

Now, we consider the network with HR neurons described by the equation of motions [7,12,14] $\dot{x} = y - x^3 + 3.0x^2 - z + 3.2, \dot{y} = 1.0 - 5.0x^2 - y, \dot{z} = 0.06[4.0(x+1.6) - z]$ and demonstrate the phenomenon of delay-enhanced stable synchronization using the MSF. The largest transverse Lyapunov exponent $\lambda_{\max}$ is depicted in Fig. 1(c) for three different τ for the network of $x(t-\tau) \to y(t-\tau)$ coupled HR neurons. For $\tau = 0$, the $\lambda_{\max}$ crosses the zero axis at $\varepsilon_{\text{thr}} = 1.43$ indicating the onset of stable synchronization and the network remains synchronized for larger ε falling into the class Γ_2. The introduction of a delay in the conjugate coupling has a tremendous effect on this scenario. With the coupling delay, the network can attain stable synchronization even well below the ε_{thr}, thereby inducing synchronization for smaller ε, and controlling the spread of stable synchronization to both an infinite (class Γ_2) and a finite (class Γ_1) range of ε for appropriate τ. This is indeed illustrated by $\lambda_{\max}$ in Fig. 1(c) for $\tau = 1.3$ and 4.9, respectively. The phenomenon of delay-enhanced stable synchronization is clearly displayed by the isoclinic lines of $\lambda_{\max} < 0$ in Fig. 2(c). The color density corresponds to the value of $\lambda_{\max}$ as shown by the color bar. It is clear from this figure that synchronization can be attained even for smaller values of ε with a delay compared to that without delay in the conjugate coupling. Further, it is also evident that in addition to extending the stable synchronized regime towards smaller values of ε, it can also remain extended to an infinite and controlled to a finite range of ε for appropriate τ in the coupling. The corresponding master stability surface, calculated using the MSF (4) for $\tau = 4.9$, depicted in Fig. 3(c) clearly indicates the stable synchronized regime by the contours of $\lambda_{\max} < 0$. The phenomenon of delay-enhanced neural synchrony was indeed demonstrated for two diffusively coupled HR neurons with $x \to x$ coupling [7]. Nevertheless, it does not establish any stable synchronized regime in the master stability surface

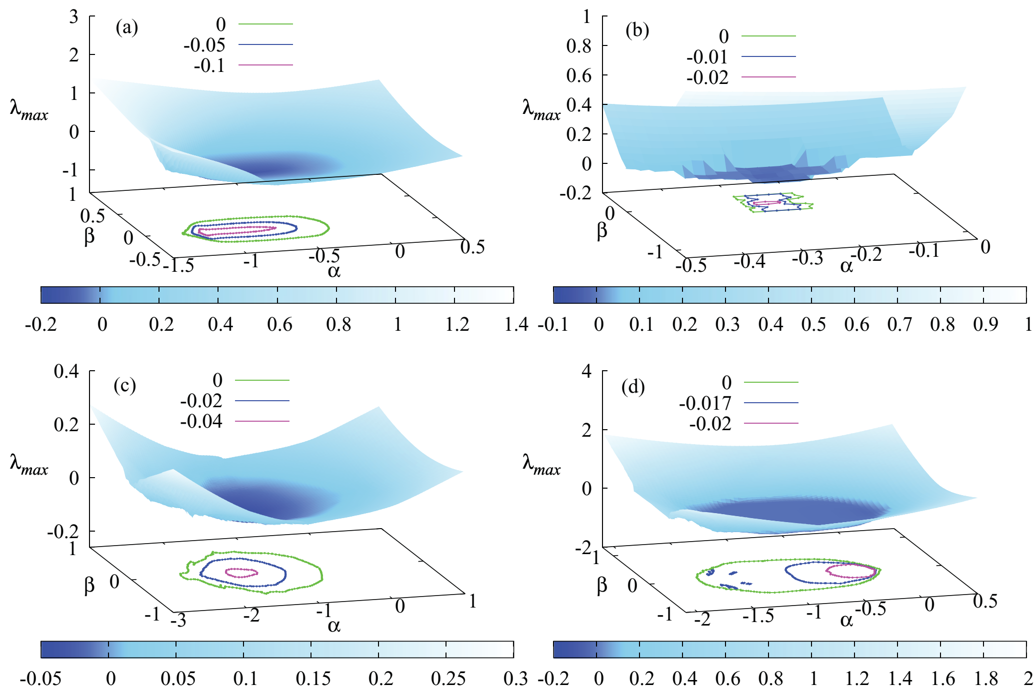

FIG. 3. (Color online) Master stability surface of the delay-coupled network. An increase in the color density corresponds to a decrease in the value of $\lambda_{\max}$ and the contours encompasses the stable synchronized regime corresponding to $\lambda_{\max} < 0$. (a) $x(t-\tau) \to y(t-\tau)$ coupled Rössler system for $\tau = 1.8$, (b) $y(t-\tau) \to x(t-\tau)$ coupled Rössler system for $\tau = 4.9$, (c) $x(t-\tau) \to y(t-\tau)$ coupled HR neurons for $\tau = 4.9$, and (d) $y(t-\tau) \to x(t-\tau)$ coupled HR neurons for $\tau = 0.8$.

using the MSF for a network of delay-coupled HR neurons with $x \to x$ coupling.

For the delayed conjugate coupling $y(t-\tau) \to x(t-\tau)$, the network of HR neurons extends the boundary of stable synchronization towards both smaller and larger values of ε illustrating the phenomenon of delay-enhanced stable synchronization. The largest transverse Lyapunov exponent estimated from Eq. (2) is shown in Fig. 1(d) for both with and without delay in the conjugate coupling. For $\tau = 0$, the stable synchronization is confined to the range $\varepsilon \in (0.28, 1.23)$ corresponding to $\lambda_{\max} < 0$, whereas the regime of stable synchronization is extended to almost twice of it for $\tau = 0.8$ in the range $\varepsilon \in (0.036, 2.31)$ in both directions of the coupling strength. This confirms the phenomenon of delay-enhanced stable synchronization in the network of HR neurons. The surface of $\lambda_{\max}$ is shown in Fig. 2(d). The contour lines, corresponding to $\lambda_{\max} < 0$ encompassing the stable synchronized regime, clearly indicate the delay-enhanced stable synchronization in the entire range of the delay we have analyzed. The corresponding master stability surface is depicted in Fig. 3(d) for the coupling delay $\tau = 0.8$. The isoclinic lines corresponding to $\lambda_{\max} < 0$ clearly assert the existence of stable synchronization in the network of HR neurons with the delayed conjugate coupling.

To summarize, we have exploited the MSF in investigating the delay effects in an arbitrary delay-coupled network with conjugate coupling. It is known that a conjugate coupling substitutes the delay coupling of the similar variable in achieving delay-induced effects. To add to its further advantage, we have shown that the delayed conjugate coupling is capable of enriching the synchronizability of the interacting dynamical systems further beyond the effects of conjugate coupling without delay. In particular, we have shown that the delayed conjugate coupling can induce stable synchronization in the network of Rössler systems, which does not exhibit any synchronous oscillations without delay in the coupling. Further, we have also shown that the delayed conjugate coupling can enhance stable synchronization to a large parameter range and it can be even achieved for smaller values of the coupling strength in the network of HR neurons compared to that without delay. The isoclinic lines of the largest Lyapunov exponents of the MSF for $\lambda_{\max} < 0$ corroborate the stable synchronization regime both in the (τ, ε) parameter space and in the complex (α, β) plane of the master stability surface. Furthermore, the delayed conjugate coupling opens up the possibility of achieving synchronization beyond the limitation on the maximum delay to be less than the time scale of the dynamical systems under consideration [10]. This may also account for the long-range neural synchrony observed in the central nervous system [7,18] as it exhibits large transmission delays (with complex topological architecture including conjugate coupling) compared to their intrinsic time scale [18], long-range spatial synchronization in ecology (for instance, synchronization of vole populations by predator birds, lynx populations) [19], in climatology (for instance, El Niño and Indian Monsoon) [20]. Currently, we are working on extending the analytics in Ref. [10] to delayed conjugate coupling to substantiate our interpretation from the phenomena of delayed conjugate coupling induced and enhanced synchronizations.

D.V.S and J.K. acknowledge the support from EU under Project No. 240763 PHOCUS (FP7-ICT-2009-C).

[1] M. Lakshmanan and D. V. Senthilkumar, *Dynamics of Nonlinear Time-delay Systems* (Springer, Berlin, 2011).
[2] H. G. Schuster and P. Wagner, Prog. Theor. Phys. **81**, 939 (1989); D. V. Ramana Reddy, A. Sen, and G. L. Johnston, Phys. Rev. Lett. **80**, 5109 (1998); D. M. Abrams and S. H. Strogatz, *ibid.* **93**, 174102 (2004); G. C. Sethia, A. Sen, and F. M. Atay, *ibid.* **100**, 144102 (2008); A. Prasad, J. Kurths, S. K. Dana, and R. Ramaswamy, Phys. Rev. E **74**, 035204(R) (2006).
[3] A. S. Pikovsky, M. G. Rosenblum, and J. Kurths, *Synchronization—A Unified Approach to Nonlinear Science* (Cambridge University Press, Cambridge, England, 2001).
[4] S. Boccaletti, J. Kurths, G. Osipov, D. L. Valladares, and C. S. Zhou, Phys. Rep. **366**, 1 (2002).
[5] A. Arenas, A. Díaz-Guilera, J. Kurths, Y. Moreno, and C. S. Zhou, Phys. Rep. **469**, 93 (2008).
[6] C. Masoller and A. C. Marti, Phys. Rev. Lett. **94**, 134102 (2005); F. M. Atay, J. Jost, and A. Wende, *ibid.* **92**, 144101 (2004); U. Ernst, K. Pawelzik, and T. Geisel, *ibid.* **74**, 1570 (1995); C. Masoller and F. M. Atay, Eur. Phys. J. D **62**, 119 (2011); J. Tang, J. Ma, M. Yi, H. Xia, and X. Yang, Phys. Rev. E **83**, 046207 (2011); Q. Wang, G. Chen, and M. Perc, PLoS ONE **6**, e15851 (2011).
[7] M. Dhamala, V. K. Jirsa, and M. Ding, Phys. Rev. Lett. **92**, 074104 (2004).
[8] L. M. Pecora and T. L. Carroll, Phys. Rev. Lett. **80**, 2109 (1998).
[9] V. Flunkert, S. Yanchuk, T. Dahms, and E. Schöll, Phys. Rev. Lett. **105**, 254101 (2010); C.-U. Choe, T. Dahms, P. Hövel, and E. Schöll, Phys. Rev. E **81**, 025205(R) (2010); A. Englert, S. Heiligenthal, W. Kinzel, and I. Kanter, *ibid.* **83**, 046222 (2011).
[10] W. Kinzel, A. Englert, G. Reents, M. Zigzag, and I. Kanter, Phys. Rev. E **79**, 056207 (2009).
[11] M. Manju Shrii, D. V. Senthilkumar, and J. Kurths, Europhys. Lett. **98**, 10003 (2012).
[12] L. Huang, Q. Chen, Y. C. Lai, and L. M. Pecora, Phys. Rev. E **80**, 036204 (2009).
[13] O. E. Rössler, Phys. Lett. A **57**, 397 (1976).
[14] J. L. Hindmarsh and R. M. Rose, Proc. R. Soc. London B **221**, 87 (1984).
[15] R. Karnatak, R. Ramaswamy, and A. Prasad, Phys. Rev. E **76**, 035201(R) (2007).
[16] A. Sharma, M. D. Shrimali, A. Prasad, R. Ramaswamy, and U. Feudel, Phys. Rev. E **84**, 016226 (2011); T. Singla, N. Pawar, and P. Parmananda, *ibid.* **83**, 026210 (2011).
[17] F. Takens, *Detecting Strange Attractors in Turbulence*, Lecture Notes in Mathematics, edited by D. Rand and L. Young, Vol. 898 (Springer, New York, 1981), pp. 366–381.
[18] F. Varela, J. P. Lachaux, E. Rodriguez, and J. Martinerie, Neuroscience (Nat. Rev.) **2**, 229 (2001); J. Fell and N. Axmacher, *ibid.* **12**, 105 (2011).
[19] R. E. Amritkar and G. Rangarajan, Phys. Rev. Lett. **96**, 258102 (2006).
[20] I. I. Mokhov, D. A. Smirnov, P. I. Nakonechny, S. S. Kozlenko, E. P. Seleznevv, and J. Kurths, Geophys. Res. Lett. **38**, L00F04 (2011).
[21] I. Fischer, R. Vicente, J. M. Buldú, M. Peil, C. R. Mirasso, M. C. Torrent, and J. García-Ojalvo, Phys. Rev. Lett. **97**, 123902 (2006).